Electronic Supplementary Information

Elucidating Phase Transformation of Eu-based Metal Organic Framework with Intermediate Isolation and Theoretical Calculation

Zhiqing Liu,[a] Ying Wu,[a] Yuan-Hui Zhong,[a] Lai-Hon Chung,*[a] Wei-Ming Liao,[a] Xianghua Yang,[a] and Jun He*[a]

[a]*School of Chemical Engineering and Light Industry, Guangdong University of Technology, Guangzhou 510006, Guangdong, P. R. China*

Correspondence to: *junhe@gdut.edu.cn*, *laihonchung@gdut.edu.cn*

General procedure.

Starting materials, reagents, and solvents were purchased from commercial sources (J&K, Zhengzhou Alfa and Acros) and used without further purification. Powder X-ray diffraction (PXRD) patterns were collected on a Rigaku Smart lab diffractometer with Cu Kα radiation (λ = 1.5418 Å) at room temperature. The X-ray tube operated at a voltage of 40 kV and a current of 15 mA. Elemental analysis (EA) was performed with a Vario Micro CUBE CHN elemental analyzer. Fourier transform infrared (FT-IR) spectra in the range 400–4000 cm^{-1} were recorded on a Nicolet Avatar 360 FT-IR spectrophotometer. Solution ^{1}H NMR spectra were recorded on a 400 MHz Bruker superconducting magnet high-field NMR spectrometer at room temperature, with tetramethylsilane (TMS) as the internal standard. Thermogravimetric analyses (TGA) were carried out in a PerkinElmer thermal analysis equipment (STA 6000).

Single crystal X-ray crystallography.

Single-crystal X-ray diffraction data of **dfdmt-INT** was collected on Rigaku Oxford Diffraction with SuperNova, Dual, Cu at home/near, Atlas diffractometer (Mo Kα, λ = 0.71073 Å with mirror as monochromator) at 240.01 K. Empirical absorption correction using spherical harmonics implemented in SCALE3 ABSPACK scaling algorithm. the **Eu-dfdmt-RB** was collected on Bruker AXS Apex II CCD diffractometer (Mo Kα, λ = 0.71073 Å with graphite as monochromator) at 296.15 K. The space group was assigned and the structure was solved by direct methods using XPREP within the SHELXTL suite of programs[1] and refined by full matrix least squares against F^2 with all reflections using Shelxl2018[2] using the graphical interface Olex2[3], which yielded the positions of all non-hydrogen atoms, and they were refined anisotropically. Hydrogen atoms were placed in calculated positions with fixed isotropic thermal parameters and included in the structure factor calculations in the final stage of full-matrix least-squares refinement. All calculations were performed using the SHELXTL system of computer programs. The treatment for the guest molecules in the cavities of all crystals involves the use of the SQUEEZE program of PLATON. Crystal data and structure refinement parameters are summarized in Table S1. Complete crystallographic data for **dfdmt-INT** and **Eu-dfdmt-RB**, in CIF format, have been deposited with the Cambridge Crystallographic Data Centre as CCDC number

2208804-2208805. These data can be obtained free of charge from The Cambridge Crystallographic Data Centre *via* www.ccdc.cam.ac.uk/data_request/cif.

Simulation details

The structures of **Eu-dfdmt-RB**, **Eu-dfdmt-B** and **dfdmt-INT** were constructed on the basis of experimental XRD data. To calculate the total energy of these structures, Density functional theory (DFT) calculations were performed using $Dmol^3$ module in Materials Studio. During the calculations, double numerical plus polarization (DNP) basis set under GGA/PW91 level of theory was used, along with different orbitals for different spins (*i.e.*, spin-unrestricted). The threshold for SCF density convergence and the maximum cycles was set to 1×10^{-6} and 500, respectively, while the octupole function was used in the multipolar representation of the charge density. To speed up the convergence, thermal smearing of 0.05 Ha was applied to the orbital occupation. Core electrons were treated by All Electron method, and a 2×2×2 k-point set was used to integrate the wavefunction.

Experimental procedures.

Synthesis of 2,5-difluoro-3,6-dimercaptoterephthalic acid (H_4dfdmt)

Organic ligand H_4**dfdmt** was synthesized according to the previously reported work.[4]

Synthesis of Eu-dfdmt-RB

H_4**dfdmt** (5.0 mg, 18.8 μmol) and $EuCl_3 \cdot 6H_2O$ (10.0 mg, 27.3 μmol) were loaded into a heavy-wall glass tube (10 mm OD, 6 mm ID), and then a solution of *N*,*N*-dimethylformamide, water and acetonitrile (0.7 mL, 4:2:1, v/v/v) was added. Then the tube was flame-sealed and heated at 140 ℃ in a programmable oven for 36 hours followed by natural cooling to room temperature and the resultant reddish-brown crystals (**Eu-dfdmt-RB**) were retrieved by filtration and washed with DMF and acetone (1.0 mL × 3), and then dried at room temperature (4.8 mg, 53.2 % yield based on H_4**dfdmt**).

Synthesis of Eu-dfdmt-B

The synthetic conditions for **Eu-dfdmt-B** was similar to **Eu-dfdmt-RB**, except that the reaction time was extended to 3 days. At the end of the reaction, **Eu-dfdmt-B** formed as black crystals upon cooling to room temperature and were collected by filtration and washed with DMF and acetone (1.0 mL × 3), and then dried at room temperature (3.2 mg, 25.2 % yield based on H_4**dfdmt**).

Synthesis of dfdmt-INT

During the growth of **Eu-dfdmt-RB** crystals, the crystals slowly dissolved and **Eu-dfdmt-B** formed. However, this transition is too fast at high temperature that no intermediate can be isolated during this process. So, by optimizing the conditions, the single crystal of the intermediate (**dfdmt-INT**) was finally obtained by the following method: After the reddish-brown crystals (**Eu-dfdmt-RB**) were formed, the mixture was further heated at the same temperature until all **Eu-dfdmt-RB** dissolved to give a clear yellow solution. Upon cooling down at this point, lots of yellow precipitates came out. After that, the mixture was reheated at 100 ℃ and all yellow precipitates dissolved to give yellow solution followed by formation of colorless crystals (**dfdmt-INT**).

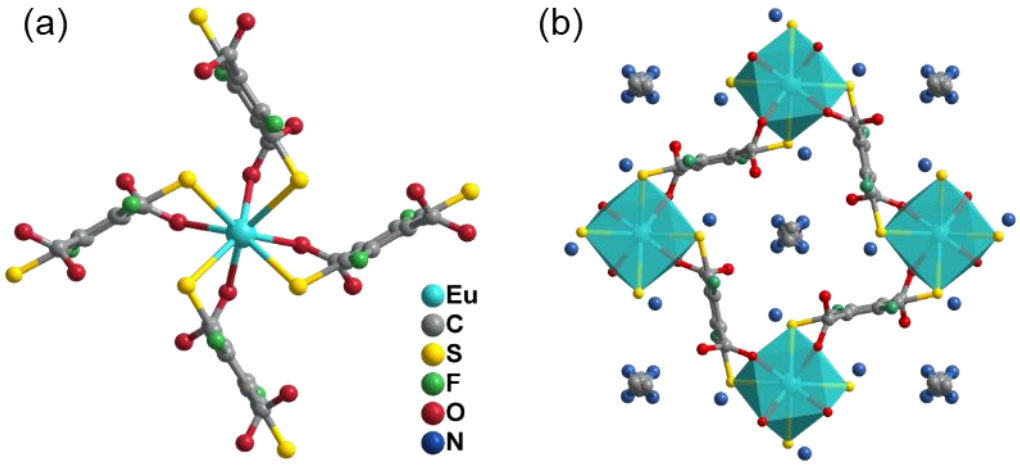

Figure S1. Single crystal structure of **Eu-dfdmt-B** (a) coordination environment of Eu, (b) a view of **Eu-dfdmt-B** and imbedded $[(CH_3)_2NH_2]^+$ and NH_4^+ (along *c* axis). H atoms are omitted for clarity.

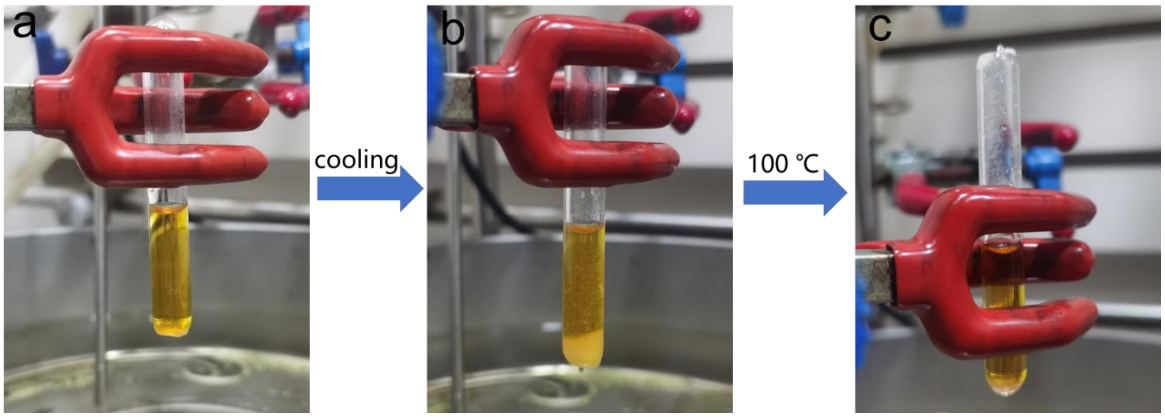

Figure S2. (a) Yellow precipitates coming from complete dissolution of **Eu-dfdmt-RB** at 140 ºC, (b) followed by rapid cooling at the state of yellow solution; (c) reheating the yellow precipitates at 100 ºC to give a yellow solution in which colorless crystals grew on the glass wall during the process.

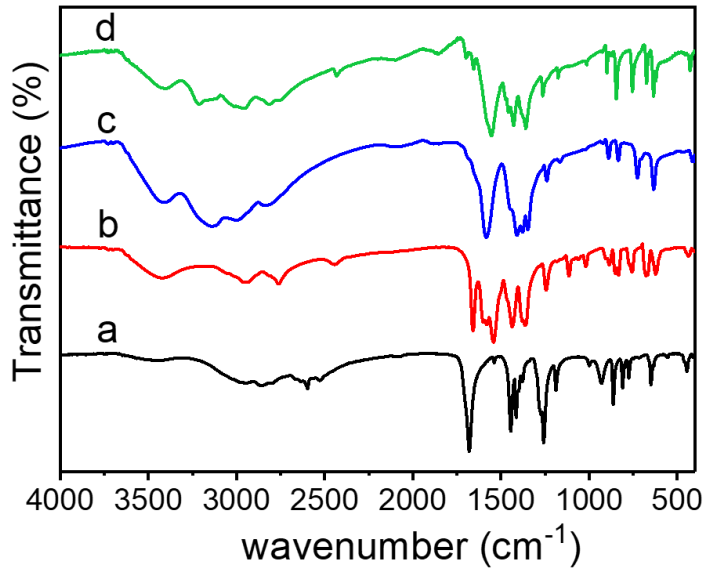

Fig. S3. The FT-IR spectra of (a) H_4**dfdmt**; (b) **Eu-dfdmt-RB**; (c) **dfdmt-INT**; (d) **Eu-dfdmt-B**.

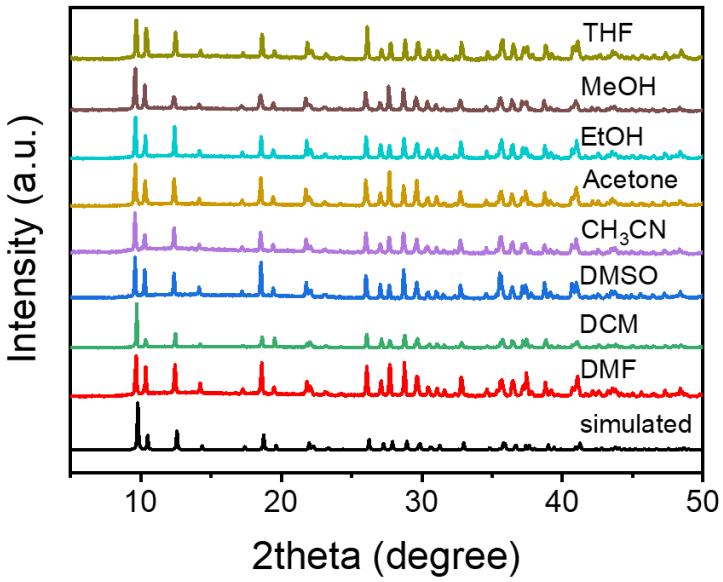

Fig. S4. PXRD patterns of **Eu-dfdmt-B** immersed in different organic solvents for 1 day.

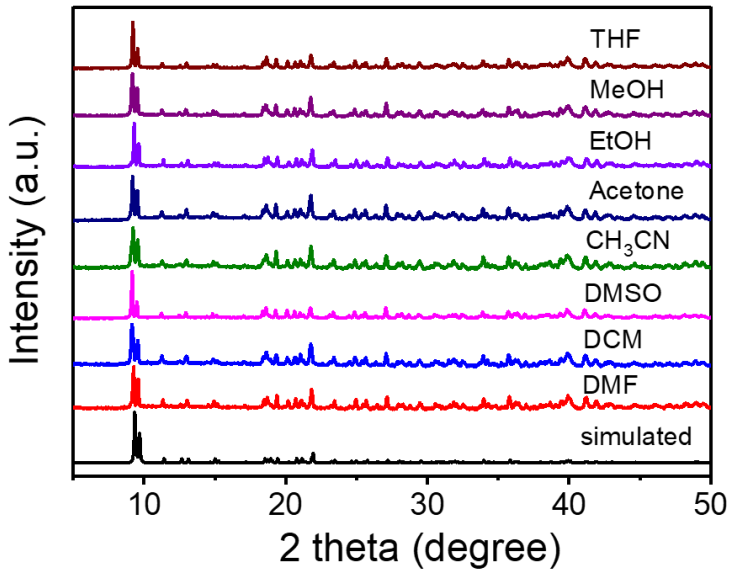

Fig. S5. PXRD patterns of **Eu-dfdmt-RB** immersed in different organic solvents for 1 day.

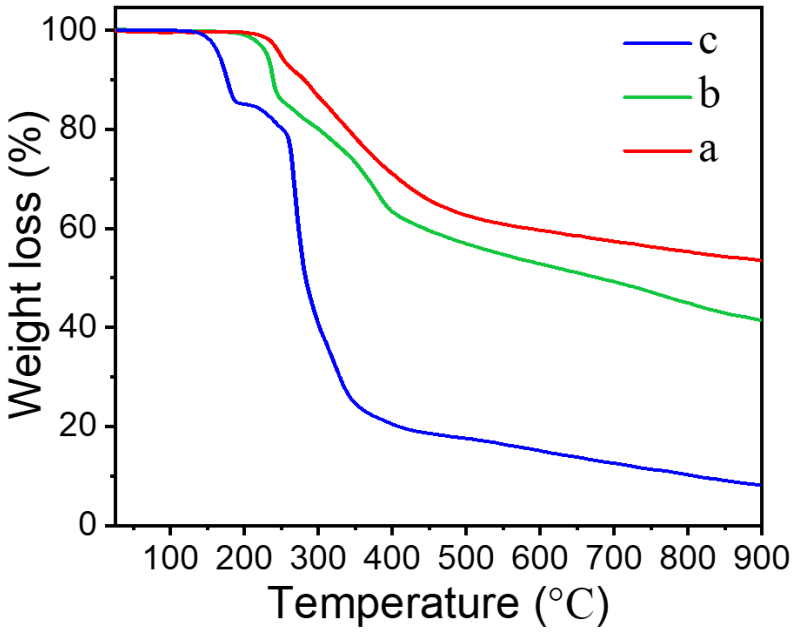

Fig. S6. The thermogravimetric analysis (TGA) plots of an activated sample of (a) **Eu-dfdmt-RB**, (b) **Eu-dfdmt-B** (c) **dfdmt-INT**.

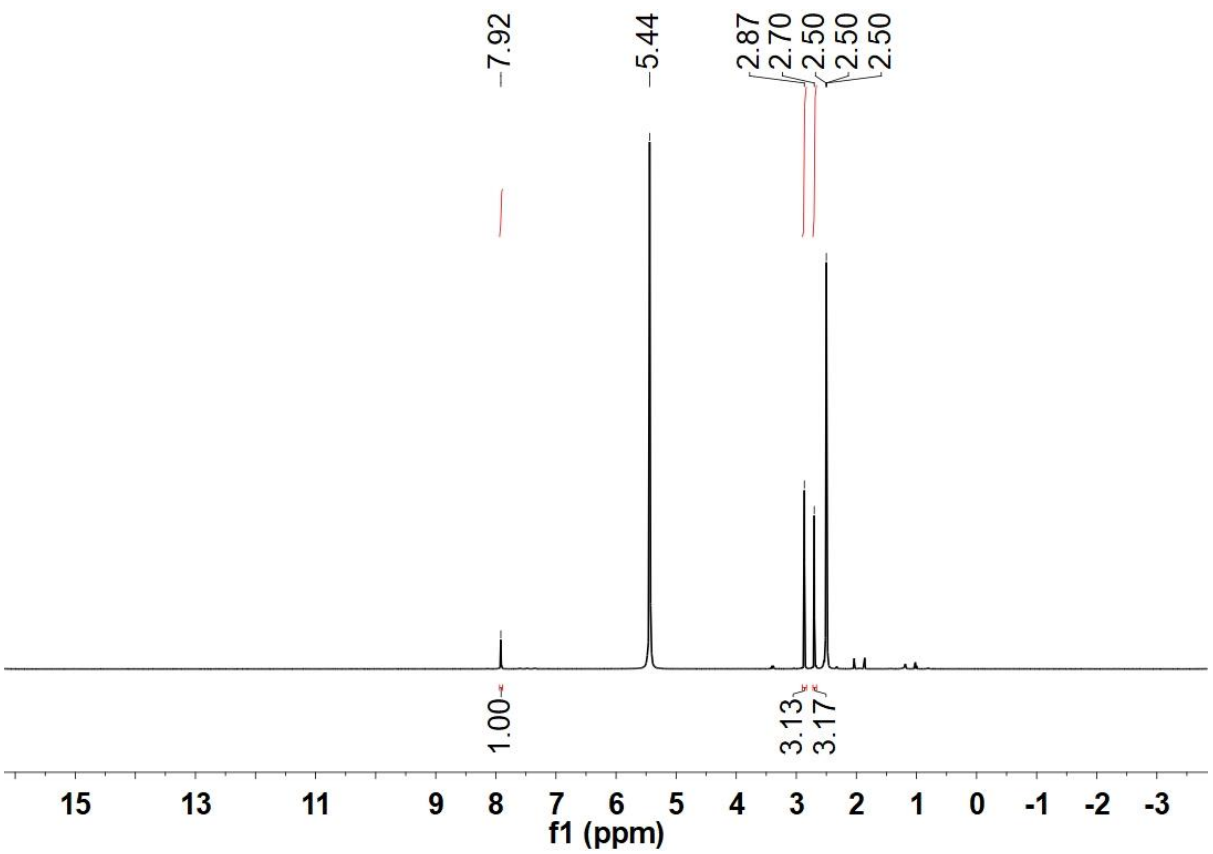

Fig. S7. A solution ^{1}H NMR spectrum of an activated **Eu-dfdmt-RB** solid (6.0 mg) dissolved in DMSO-d_6 (0.5 mL)/DCl (38 % in D_2O, 0.02 mL).

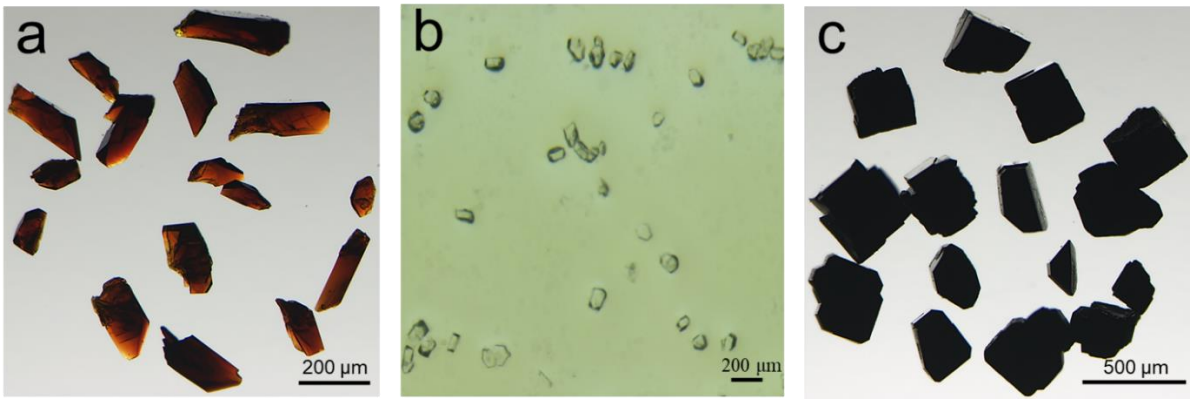

Fig. S8. The optical microscopic photograph of (a) **Eu-dfdmt-RB**, (b) **dfdmt-INT** and (c) **Eu-dfdmt-B.**

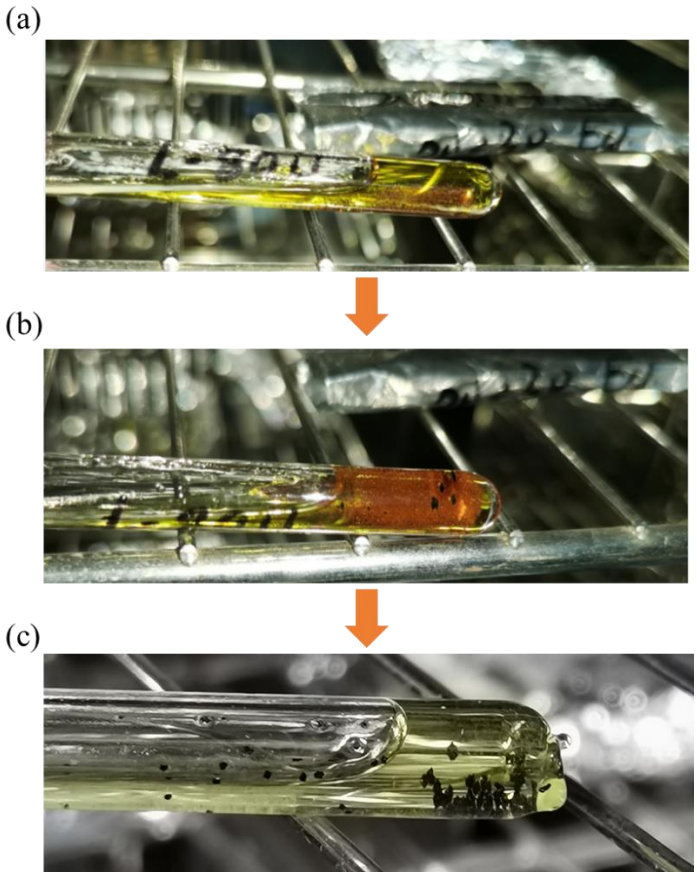

Fig. S9. Phase transition process from **Eu-dfdmt-RB** to **Eu-dfdmt-B**. a) **Eu-dfdm-RB** begins to be generated, b) **Eu-dfdmt-RB** and **Eu-dfdmt-B** coexist, c) **Eu-dfdmt-RB** disappears to form **Eu-dfdmt-B**.

Table S1. Crystallographic data and refinement results for **Eu-dfdmt-RB** and **dfdmt-INT**.

Compound name	**Eu-dfdmt-RB**	**dfdmt-INT**
Empirical formula	$C_{11}H_7EuF_2NO_5S_2$	$C_8H_{18}F_2N_4O_5S_2$
Formula weight	487.26	352.38
Temperature/K	293(2)	240(10)
Crystal system	Triclinic	Monoclinic
Space group	$P\bar{1}$	$P2_1/c$
a/Å	9.4105(14)	16.6143(5)
b/Å	9.5147(14)	10.5019(3)
c/Å	9.8831(15)	8.8283(3)
α/°	106.078(2)	90.00
β/°	94.529(2)	103.725(4)
γ/°	92.030(2)	90.00
V/Å^3	846.12(2)	1496.38(8)
Z	2	4
D_c/g·cm^{-3}	1.912	1.564
μ/mm^{-1}	3.990	0.404
F(000)	466	736
R_1[a][$I>2\sigma(I)$]	0.0254	0.0306
wR_2[b](all data)	0.0658	0.0841
GOF	1.042	1.068

[a]$R_1=\sum(||F_0|-|F_c||)/\sum|F_0|$; [b]$wR_2=[\sum w(F_0^2-F_c^2)^2/\sum w(F_0^2)^2]^{1/2}$

References:

1. G. M. Sheldrick, *Acta Crystallogr. A,* 2008, **64**, 112-122.
2. G. M. Sheldrick, *Acta Crystallogr. C Struct. Chem.*, 2015, **71**, 3-8.
3. O. V. Dolomanov, L. J. Bourhis, R. J. Gildea, J. A. K. Howard and H. Puschmann, *J. Appl. Crystallogr.*, 2009, **42**, 339-341.
4. Q. Zeng, L. Wang, Y. Huang, S. L. Zheng, Y. He, J. He, W. M. Liao, G. Xu, M. Zeller and Z. Xu, *Chem. Commun.*, 2020, **56**, 3645-3648.